PCCP

ROYAL SOCIETY OF CHEMISTRY

PERSPECTIVE

View Article Online
View Journal | View Issue

Check for updates

Cite this: *Phys. Chem. Chem. Phys.*, 2023, **25**, 23370

The role of small molecular cations in the chemical flow of the interstellar environments

Lola González-Sánchez, *[a] N. Sathyamurthy [b] and Francesco A. Gianturco [c]

Received 26th June 2023,
Accepted 15th August 2023

DOI: 10.1039/d3cp03000h

rsc.li/pccp

Molecular ions have been ubiquitous in a variety of environments in the interstellar medium, from Circumstellar Envelopes to Dark Molecular Clouds and to Diffuse Clouds. Their role in the multitude of molecular processes which have been found to occur in those environments has been the subject of many studies over the years, so that we have acquired by now a complex body of data on their chemical structures, their possible function within chemical reactions and their most likely paths to formation. In the present work we review a broad range of such molecular ions, focusing exclusively on positive ions involving the smallest and simplest cations which have been either detected or conjectured as present in the interstellar medium (ISM). We therefore consider mainly molecular cations formed with components like H, H^+, He and He^+, atomic species which are by far the most abundant baryons in the ISM in general. Their likely structures and their roles in a variety of chemical energy flow paths are discussed and presented within the context of their interstellar environments.

Open Access Article. Published on 17 August 2023. Downloaded on 09.08.2025 04:28:18.
This article is licensed under a Creative Commons Attribution-NonCommercial 3.0 Unported Licence.

1 Introduction

Most of the matter in the universe is localized into large gatherings of stars known as galaxies. In most of the galaxies that can be studied by direct observation, the space between stars is found to be frequently occupied by a variety of material that contains the so-called interstellar clouds, which in turn consist of gas and dust and are embedded in a more rarefied medium. Densities and temperatures of interstellar clouds vary widely, and indeed few clouds are homogeneous. The simplest clouds are known as "diffuse" since the gas and dust in such regions is not dense enough to keep out starlight, so that astronomical observations can detect diffuse material in between the bright stars and our position. Typical temperatures of such regions are in the vicinity of 50–100 K and total gas densities are perhaps of the order of 10^2 cm^{-3}.[1] As in all interstellar clouds, the gas is mainly hydrogen, betraying the fact that the material in clouds comes from previous generation of stars, which are also mainly hydrogen in content. Some average "cosmic" elemental abundances, normalized with respect to hydrogen, and taken from the atmospheres of nearby stars, have also been reported in the literature.[2] The heavy elements in stars are found to be depleted in interstellar gas because they also constitute the dust particles which are mainly silicates and carbonaceous material. By mass, the dust is typically 1% of the gas, and consists of particles ranging widely in radius from $\leq$10 nm to more than 1 μm. A standard size often quoted by astronomers is 0.1 μm.[3]

Although the gas phase in diffuse clouds is mainly neutral, virtually all of the carbon is ionized by ultra-violet radiation from stars, leading to a fractional ionization of about 10^{-4}.[1] The more abundant elements, which are H and He, cannot be ionized by stellar ultra-violet radiation because it does not extend to high enough energies, terminating at 13.6 eV, the ionization potential of atomic hydrogen. Some ionization of these abundant atoms comes from cosmic rays, which are mainly protons traveling at relativistic speeds. The hydrogen is typically divided evenly between neutral atomic and molecular forms and it is thought that the molecules are produced not in the gas but *via* recombination on the surfaces of dust particles. Other than molecular hydrogen, all molecules are trace constituents of the gas. Until recently, it was thought that only diatomic species (*e.g.* CH, CN, OH, NH, C_2) were present in diffuse clouds but the situation is now known to be more complex and includes several ionized molecules and also a fairly large variety of polyatomic molecules. The most prominent molecular ion detected is CH^+, which can be seen *via* its visible spectrum. This ion possesses a fractional abundance of only 10^{-7}, far below that of C^+.

The chemistry that occurs in the dense interstellar gas is considered to be far more complex than that assumed to occur in the diffuse gas. Dense gas is normally associated with giant molecular clouds, which are large heterogeneous assemblies of

[a] *Departamento de Química Física, University of Salamanca, Plaza de los Caídos sn, 37008 Salamanca, Spain. E-mail: lgonsan@usal.es*
[b] *Indian Institute of Science Education and Research Mohali, SAS Nagar, Punjab 140306, India*
[c] *Institut für Ionenphysik und Angewandte Physik, Universität Innsbruck, Technikerstr. 25, 6020, Innsbruck, Austria*

 This journal is © the Owner Societies 2023

Open Access Article. Published on 17 August 2023. Downloaded on 09.08.2025 04:28:18.
This article is licensed under a Creative Commons Attribution-NonCommercial 3.0 Unported Licence.

gas and dust ranging in mass up to about 10^5 solar masses. The dense portions, virtually black in the visible region, are known as 'cores' and have typical temperatures of only 10 K and densities of about 10^4 cm^{-3}, consisting by their major parts of molecular rather than atomic hydrogen.[4] Although some cores are termed 'quiescent', others are actively collapsing to form stars. The detection of molecules in regions of active star formation tells us much about the physical conditions and their evolution. The earliest active stage of stellar evolution is known as a pre-stellar core; here the collapse is still isothermal but a condensation of higher density begins to form in the center as collapse occurs. In this denser region within a core, heavy molecules condense out onto the surfaces of dust particles to form mantles of ices, and the gas becomes almost completely hydrogen and helium. In the next stage, known as a protostellar core and subdivided into various categories, the collapse turns adiabatic in the center and a warm 'protostar' develops. Near the star's location the dust grains can become warmer so that the mantles can evaporate and return to the gas.[3]

The result of the above sketch on the evolutionary aspects of interstellar clouds is that a broad variety of molecular species can be present, and have been observed, in both translucent and dark molecular clouds and that many of the observed species have been molecular ions, especially cations, produced often by starlight ionization of the corresponding neutrals. It is the aim of the present perspective article to discuss a series of small molecular cations which have been observed in the Interstellar Medium (ISM) and to evaluate their efficiencies in transferring various forms of energies to other partners. The latter will be obviously the most abundant ISM components and therefore we will discuss, whenever possible, collision energy transfer probabilities with He, H and H_2 as the likely partners and under the expected features of that environment. Since under the very special conditions of what is termed as the early universe, the formations of cations are also considered the only viable molecular paths, we will discuss in detail the role of the first molecule suggested to have been existing at that redshift: the HeH^+ cation and also the H_3^+, the simplest polyatomic molecular cation. Additionally, the possible presence of heavier baryon species like LiH^+ and $LiHe^+$, of small C-bearing cations and of cations with higher metalicity will also be briefly discussed.

2 Cations in the interstellar medium

Even before molecular ions were detected in dense interstellar clouds, it was suggested that ions must play a prominent role in the chemistry occurring in the gas-phase since, especially in the cold regions, the dominant processes should be, in order to be effective, exothermic reactions that have no activation energy.[5] Indeed, unlike most neutral–neutral reactions, ion–molecule reactions often do not possess activation-energy barriers, or energy barriers along the Transition State (TS) formation, and so can play a significant role within the interstellar chemical networks despite the existence, as we have discussed earlier, of the low fractional ionization in dense clouds. The primary ion in dense clouds is H_3^+, because it is expected to be made early on in the reaction chain and can serve as a precursor for the formation of more complex species.[6] Molecular hydrogen is formed on the surfaces of grains, and is released to the gas either during the reaction or by evaporation. Ionization is caused by encounters with cosmic rays, typically with relativistic energies of 100 MeV or more, which lead mainly to the removal of a single electron and the formation of H_2^+.[5] This ion reacts "immediately" (within a day) with molecular hydrogen, the dominant species, to form the H_3^+ ion.[7] The H_3^+ does not react with H_2 and so is relatively abundant. Since it does not possess a permanent dipole moment, it does not exhibit a strong rotational spectrum and therefore remained undetected for a long time, until technological improvements in infra-red sensitivity led to its observation in this spectral region. The observed abundance of this special cation in dense clouds turned out to be what had been predicted, as it will be further discussed below. Another primary ion is He^+, formed by cosmic ray bombardment of abundant helium atoms, and also often considered to be largely unreactive with H_2.[5]

Among the many molecules detected in diffuse and dense gas clouds the positive molecular ions involve simple diatomics like CH^+, CO^+ and SH^+, triatomic partners like H_3^+ and its isotopic variants, HCO^+, HN_2^+, and HCS^+. Those found in diffuse clouds include the classic CH^+, mentioned above, as well as H_3^+ and HCO^+. The latter two are more strongly associated with dense gas while the other ions mentioned are only found in denser material. The ion HCO^+ is associated especially with the Photon-Dominated Regions (PDRs) and the isomer HOC^+ has also been recently detected in such regions. The presence of deuterated ions is an important indicator of the physical conditions in star formation regions, especially pre-stellar cores. The most abundant molecular ion in dense sources is, as can be seen in the reference quoted below, the HCO^+ cation, except for the cold pre-stellar cores where virtually all non-hydrogenic material is frozen out. An estimated fractional ionization in dense cores is considered to be around 10^{-7}, as discussed in ref. 5.

The presence of the smaller molecular variants of diatomic or triatomic cations is particularly intriguing since their relative structural simplicity indicates that their abundances can be observed within different environments, thereby suggesting their significant participation to energy-transfer dynamics activated by collisions with the other abundant neutral partners like H, He and H_2. In the following Sections we shall therefore discuss in greater details just how much such collision events can provide significant probabilities for energy flow rate coefficients at the temperatures of interest in the interstellar environments.

The subject of molecular ions in extraterrestrial space has grown in the last several decades, with a large number of cationic and anionic species detected in the ISM regions. Since there are several reviews on the subject,[8–10] we shall not attempt a complete presentation here, but confine ourselves to

Open Access Article. Published on 17 August 2023. Downloaded on 09.08.2025 04:28:18.
This article is licensed under a Creative Commons Attribution-NonCommercial 3.0 Unported Licence.

a perspective that will focus on the general features of lighter species of low atomic number, and composed of only a few atoms. Such components are in fact more likely to have formed in the early universe as well as in the later interstellar media. Not surprisingly, many of them are hydrogen/helium containing species.

3 HeH^+ and its energy exchanges with H, He and H_2 as partners

At the beginning of the chemical epoch of the early universe, there were protons (H^+) and α particles (He^{++}) in the ratio 1 : 0.1 with small amounts of D^+ and Li^{3+}.[11,12] Energetics[13] favored the formation of He, the first neutral atom to be formed in the early universe:

$$He^{++} + e \rightarrow He^+, \quad \Delta E = -54.418 \text{ eV} \qquad (1)$$

$$He^+ + e \rightarrow He, \quad \Delta E = -24.584 \text{ eV} \qquad (2)$$

Thus,

$$He^{++} + 2e \rightarrow He, \quad \Delta E = -79.002 \text{ eV} \qquad (3)$$

in contrast to

$$H^+ + e \rightarrow H, \quad \Delta E = -13.598 \text{ eV} \qquad (4)$$

Understandably, He atoms would have combined with the abundant H^+ to form the first diatomic species HeH^+ by radiative association (RA) in the early Universe:[14,15]

$$He + H^+ \rightarrow HeH^+ + h\nu, \quad \Delta E_0 = -1.84 \text{ eV} \qquad (5)$$

It is worth pointing out at this stage that it is practically impossible to measure the rate coefficient (k) for RA under laboratory conditions because they require fairly low concentration of the relevant species $\sim 10^2$ cm^{-3} in order for them to mimic early universe conditions. Therefore, we would have to rely on theoretical estimates. The values of the k_{RA} for reaction (5) were estimated to vary from 6.42×10^{-20} cm^3 $molecule^{-1}$ s^{-1} at 2 K to 0.56×10^{-20} cm^3 $molecule^{-1}$ s^{-1} at 10 000 K, with a maximum of 13.25×10^{-20} cm^3 $molecule^{-1}$ s^{-1} at 18 K,[16] thus confirming the generally small probabilities that such processes would have.

Although HeH^+ was detected in a mass spectrograph[17] as early as 1925, concrete spectroscopic evidence for its presence in the planetary nebula NGC 7027 came only recently.[18,19] Interestingly, the mechanism for its formation in interstellar medium (ISM) was suggested to be

$$He^+ + H \rightarrow HeH^+ + h\nu, \quad \Delta E_0 = -12.824 \text{ eV} \qquad (6)$$

because of the abundance of H in interstellar clouds. In addition, k_{RA} for reaction (6) has been estimated to be 9.93×10^{-15} cm^3 $molecule^{-1}$ s^{-1} at 1 K, decreasing monotonically to 1.01×10^{-15} cm^3 $molecule^{-1}$ s^{-1} at 4000 K;[20] $k_{RA} = 5.68 \times 10^{-15}$ cm^3 $molecule^{-1}$ s^{-1} at 10 K, decreasing to 0.77×10^{-15} cm^3 $molecule^{-1}$ s^{-1} at 4000 K.[21]

The reaction of He^+ with the more abundant H_2 does not seem to lead to the formation of HeH^+ because of a large barrier arising from the potential energy surfaces of two states of the same symmetry avoiding crossing each other.[22] On the other hand, the dissociative charge transfer (DCT) reaction

$$He^+ + H_2 \rightarrow He + H + H^+, \quad \Delta E_0 = -6.5 \text{ eV} \qquad (7)$$

seems to actually occur.[23] As a matter of fact, Schauer *et al.*[24] measured the k for the radiative charge transfer (RCT)

$$He^+ + H_2 \rightarrow He + H_2^+, \quad \Delta E_0 = -9.16 \text{ eV} \qquad (8)$$

and the dissociative charge transfer in $He^+ + H_2$ collisions in the temperature range 15–40 K in an ion trap. While k_{RCT} was found to be of the order of 1×10^{-14} cm^3 $molecule^{-1}$ s^{-1} and independent of temperature, k_{DCT} was found to increase in the range $2.5–5 \times 10^{-14}$ cm^3 $molecule^{-1}$ s^{-1} as T increased from 15 to 40 K.

In a measurement of the dissociative recombination (DR) rate coefficients for HeH^+

$$HeH^+ + e \rightarrow He + H \qquad (9)$$

in an ion storage ring, Novotny *et al.*[25] found these coefficients to be much smaller than what was expected from earlier investigations, thereby suggesting that HeH^+ is much more abundant in astrochemical environment than previously expected. Forrey *et al.*[26] and Courtney *et al.*[27] took stock of the factors responsible for the formation of HeH^+ in planetary nebulae as well as in the early Universe and concluded that HeH^+ was at least three orders of magnitude more abundant than what was predicted earlier for the larger redshifts (z) near 20.

HeH^+ can also get destroyed by the reactions

$$HeH^+ + H \rightarrow He + H_2^+, \quad \Delta E_0 = -0.80 \text{ eV} \qquad (10)$$

and

$$HeH^+ + H_2 \rightarrow He + H_3^+, \quad \Delta E = -2.63 \text{ eV} \qquad (11)$$

Both the molecular events are exothermic and barrierless.

Karpas *et al.*[28] had determined the k for the reaction (10) to be $(9.1 \pm 2.5) \times 10^{-10}$ cm^3 $molecule^{-1}$ s^{-1} at 300 K. Adams *et al.*[29] had estimated the k for the reaction (11) to be $\geq 3.5 \times 10^{-11}$ cm^3 $molecule^{-1}$ s^{-1} at 200 K (~ 0.017 eV). Ryan and Graham[30] measured it to be $(1.4 \pm 0.2) \times 10^{-9}$ cm^3 $molecule^{-1}$ s^{-1} at a mean energy of 0.1 eV. Rutherford and Vroom[31] estimated it to be 2.3×10^{-9} cm^3 $molecule^{-1}$ s^{-1} at E_{trans} = 0.3 eV. They also reported the cross section for the reaction to be 38 $Å^2$ at E_{trans} = 0.3 eV, decreasing to 1 $Å^2$ at E_{trans} = 6 eV. The rate of decay of the cross section with E_{trans} in the range 0.4–2 eV was as predicted by Gioumousis and Stevenson.[32] Johnsen and Biondi[33] determined the k to be $\geq 10^{-9}$ cm^3 $molecule^{-1}$ s^{-1} at 300 K. Subsequently, Orient[34] measured it to be $(1.26 \pm 0.16) \times 10^{-9}$ cm^3 $molecule^{-1}$ s^{-1} at 300 K and independent of E_{trans} in the range 0–0.3 eV. This is somewhat smaller than what was reported (1.8×10^{-9} cm^3 $molecule^{-1}$ s^{-1}) earlier by Theard and Huntress.[35]

In the case of HeH^+ colliding with He, the potential energy surface has a well of depth of 0.578 eV as revealed by the

 This journal is © the Owner Societies 2023

Open Access Article. Published on 17 August 2023. Downloaded on 09.08.2025 04:28:18.
This article is licensed under a Creative Commons Attribution-NonCommercial 3.0 Unported Licence.

existing *ab initio* calculations.[36] Bound state calculations have also shown that the potential well can support several bound states.

$$HeH^+ + He \rightarrow [He_2H^+] \rightarrow HeH^+ + He \qquad (12)$$

In addition to the reactive events mentioned above, HeH^+ can undergo rotational-vibrational inelastic state-changes due to collision with He, H and H_2. While Desrousseaux and Lique[37] reported the rotational inelastic cross sections for HeH^+ due to collision with H, the present authors reported the relevant cross sections and rate coefficients for the rotational inelastic transitions due to collision with He and H_2.[38,39] It is worth adding at this point that rotational and vibrational inelastic transitions can have a reactive as well as a nonreactive component in the case of (HeH^+, He) and (HeH^+, H) collisions, although both the components are indistinguishable in a real detection, albeit present from quantum calculations. It was therefore found from such calculations that H_2 is more efficient than He and H in causing rotational excitations in HeH^+ as illustrated in the example from our calculations, reported here in Fig. 1.[39] It is important to add that vibrational inelastic transitions in HeH^+ have an order of magnitude lower k values when compared with the pure rotationally inelastic paths.[40]

It also turns out that the Dissociative Recombination (eqn (9)) has a much higher rate coefficient of $\sim 10^{-7}$ cm^3 molecule^{-1} s^{-1}.[41] A qualitative, pictorial summary of the formation and destruction routes for HeH^+ and its relation with other atomic and molecular species is given in Fig. 2.

Gianturco and coworkers have shown that HeH^+ could nucleate several helium atoms around it,[42] although clusters larger than He_2H^+ are unlikely to be formed under ISM conditions because of the much more diluted presence of the involved partners.

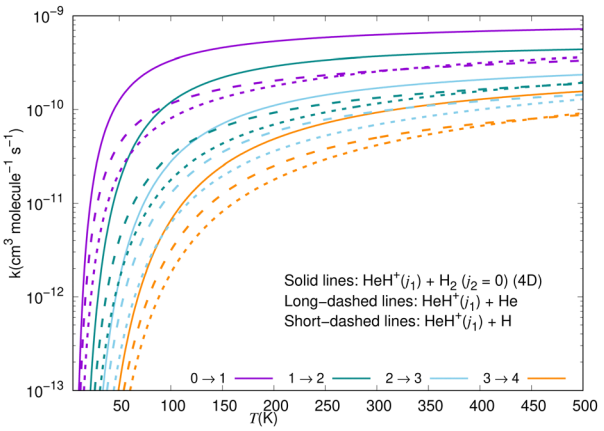

Fig. 1 Computed (Δj_1 = +1) excitation rate coefficients for a series of inelastic processes in HeH^+ (j_1) + p-H_2 (j_2 = 0) collisions[39] (solid lines), compared with the corresponding results for HeH^+ + He[38] (long-dashes) and HeH^+ + H collisions[37] (short-dashes). Adapted from Fig. 21 of ref. 39.

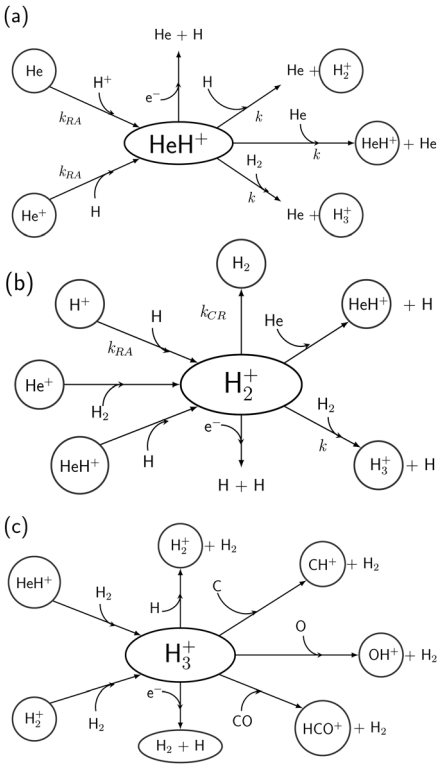

Fig. 2 A pictorial view of the interconnections between He, H, H_2 and the related ionic molecular species. Formation and destruction channels for (a) HeH^+, (b) H_2^+ and (c) H_3^+.

4 H_2^+ and its isotopomers: dynamics with He as a collision partner

In the early universe, H_2^+ was presumably formed by radiative association

$$H + H^+ \rightarrow H_2^+ + h\nu, \quad \Delta E_0 = -2.65 \text{ eV} \qquad (13)$$

In addition, it was likely to be formed by proton transfer reaction (10). In interstellar clouds, however, H_2^+ seems more likely to be formed by ionization of H_2 by cosmic radiation.[9] H_2^+ could also be formed by the radiative charge transfer (RCT) process:

$$He^+ + H_2 \rightarrow He + H_2^+ + h\nu \qquad (14)$$

Mrugala and Kraemer[43] estimated the k_{RCT} for the above process to be between 2.5 and 3.5 times larger than the experimental results (1–1.1) $\times$ 10^{-14} cm^3 molecule^{-1} s^{-1} at 15–35 K and $\sim 7.5 \times 10^{-15}$ cm^3 molecule^{-1} s^{-1} at 40 K.[24]

In the early Universe, H_2^+ was, presumably, also responsible for H_2 formation:

$$H_2^+ + H \rightarrow H_2 + H^+ \qquad (15)$$

Karpas *et al.*[28] determined the k to be (6.4 $\pm$ 1.2) $\times$ 10^{-10} cm^3 molecule^{-1} s^{-1} at 300 K.

H_2^+ could also be destroyed by reaction with H_2:

$$H_2^+ + H_2 \rightarrow H_3^+ + H, \quad \Delta E_0 = -1.7 \text{ eV} \qquad (16)$$

Open Access Article. Published on 17 August 2023. Downloaded on 09.08.2025 04:28:18.
This article is licensed under a Creative Commons Attribution-NonCommercial 3.0 Unported Licence.

The k value for the latter reaction was found to be 2.11×10^{-9} cm^3 molecule^{-1} s^{-1} at 300 K.[28] The inelastic collisions between H_2^+ and He have been investigated by Gianturco and collaborators[44] and we shall be discussing it below.

The reaction of H_2^+ with He is highly endothermic:

$$H_2^+ + He \rightarrow [HeH_2^+] \rightarrow HeH^+ + H, \quad \Delta E_0 = 0.80 \text{ eV} \tag{17}$$

It is also worth mentioning that this was the first ion–molecule reaction for which vibrational enhancement was demonstrated experimentally.[45,46] The reaction as well as the inelastic collisions between H_2^+ and He are influenced by the presence of a potential well (see below). The literature on the system has been reviewed recently.[22]

We briefly mention again at this point that Vera *et al.*[44] computed the rotationally inelastic integral cross sections for *p*- and *o*-H_2 ($v = 0$) colliding with He for E_{trans} in the range 1–1000 cm^{-1} and rate coefficients for T in the range 1–100 K. While the $0 \rightarrow 2$ ($6B_e$) rotational excitation cross section for *p*-H_2^+ rose from the threshold to a maximum of $\sim$20–25 Å^2, and showed several narrow peaks, the $1 \rightarrow 3$ ($10B_e$) excitation cross section for *o*-H_2^+ rose to a maximum of 15 Å^2. On the other hand, all other excitation cross sections turned out to be considerably smaller. These differences were readily attributed to the difference in the anisotropic coupling terms of their inelasic PES and also to the existence of an exponential decrease in the cross sections with an increase in the energy gaps between the involved states in the relevant transition.[47,48] The corresponding rate coefficients determined by the recent calculations[44] were found to be at the most of $\sim 10^{-10}$ cm^3 molecule^{-1} s^{-1} at 100 K while they were orders of magnitude smaller at lower T. The vibrational excitation cross section values obtained by Iskandarov *et al.*[49] using the same PES[50] were an order of magnitude smaller for *p*-H_2^+–He collisions, thus confirming the differences which exist between the two energy-transfer processes in term of their nanoscopic coupling mechanisms and as discussed in the above references.

Since optical excitation/de-excitation of H_2^+ and D_2^+ to different ro-vibrational states is not possible, Schiller *et al.*[51] showed, by using quantum scattering calculations, that rotationally cooled H_2^+ (20 K) and D_2^+ (40 K) could, in principle, be produced in the laboratory using cold He as the buffer gas. In another simulation carried out by the same authors, and also using quantum scattering calculations, Vera *et al.*[52] showed from computational simulations that differential reaction cross sections for the reaction (17), in case were to be experimentally obtained in future experiments, could be measured by using velocity mapping tools and the results would be sensitive to the initial ro-vibrational state selection for H_2^+. Thus, one can in principle surmise that reactivity for state-selected initial partners could also become amenable to experimental observations.

Although deuterium is an isotope of hydrogen, astrophysical models treat the former as a separate element. Isotopically substituted H_2^+, *i.e.* HD^+ has a special role to play in the cooling of stellar gases because of its asymmetry and the resultant dipole moment, a feature making both radiative and collisionl interactions more likely to occur. Therefore, for that same reason, HD^+ is formed more readily than H_2^+ by radiative association, a property confirmed by calculations.

Furthermore, one sees that there is a difference in reactivity between the H-end and the D-end in the reaction of HD^+ with He and other atomic and molecular species, as discussed, for example, in ref. 53. We are not going to discuss the isotopic variants here because the abundance of HD^+ is found to be several orders of magnitude lower than that of H_2^+. Such marked changes in column densities, therefore, are preventing the isotopic variants to work as effectively as their lighter counterparts in participating in the chemical networks where such molecular cations are deemed to be present. Hence, although they are often discussed in the current literature for completeness, we will not analyse them any further in the present perspective.

5 HeH_2^+: structure and chemical energy flows

As mentioned earlier, Mrugala *et al.*[54] estimated the k_{RA} to have a maximum value of 2.1×10^{-20} cm^3 molecule^{-1} s^{-1} at about 20 K for the formation of HeH_2^+ from He and H_2^+:

$$He + H_2^+ \rightarrow HeH_2^+ + h\nu \tag{18}$$

These authors (*e.g.* see: Mrugala and Kraemer[43]) further estimated the k_{RA} to have a maximum value of 3.3×10^{-15} cm^3 molecule^{-1} s^{-1} around 2 K for the complementary route of formation of HeH_2^+:

$$He^+ + H_2 \rightarrow HeH_2^+ + h\nu \tag{19}$$

As it was mentioned earlier, HeH_2^+ was detected in a mass spectrograph in 1925, but its microwave spectrum near its dissociation limit was recorded only in 1996 by Carrington *et al.*[55,56] There was a sharp doublet around 21.8 GHz (0.73 cm^{-1}), which was attributed to [*p*-H_2–He]$^+$ with the possibility of He being at either end of H_2^+. There was a sextet around 15.2 GHz (0.51 cm^{-1}), which was attributed to [*o*-H_2–He]$^+$, the higher multiplicity arising from the nuclear magnetic moment ($I = 1$) of *o*-H_2^+.[57,58]

Ab initio calculations[22] had suggested that HeH_2^+ could be stable by 0.34 eV, relative to the well separated He and H_2^+. Kraemer *et al.*[21] had shown that there could be a shallower potential well of -0.145 eV in the first excited state. Hopper[59] had suggested that the (He^+, H_2) collision could result in radiative association and form HeH_2^+, with concomitant emission at 153 nm.

Meuwly and Hutson[57] had suggested associative ionization

$$He^* + H_2 \rightarrow [HeH_2^+] + e \tag{20}$$

as a possible means of formation of HeH_2^+. Some of us have suggested recently that it could be formed due to non-adiabatic coupling terms acting like friction.[60]

 This journal is © the Owner Societies 2023

Open Access Article. Published on 17 August 2023. Downloaded on 09.08.2025 04:28:18.
This article is licensed under a Creative Commons Attribution-NonCommercial 3.0 Unported Licence.

The vibrational spectrum of HeH_2^+ and HeD_2^+ in an ion trap at 4 K was reported recently by Asvany *et al.*[61] Based on the results of their variational calculations for the ro-vibrational bound states on the 3D PES reported by Koner *et al.*,[62] Asvany *et al.* assigned the peak at 1840 cm^{-1} to the H–H fundamental stretch and the peaks at 632 and 732 cm^{-1} to the H_2^+–He bend and stretch, respectively; The corresponding peaks for HeD_2^+ occur around 1309, 473 and 641 cm^{-1}, respectively.

It is hoped that HeH_2^+ will be detected soon in ISM.

6 He_2^+: processes with H as a collision partner

It is considered to be likely[15] that He_2^+ was formed early on by radiative association

$$He + He^+ \rightarrow He_2^+ + h\nu \quad (21)$$

although it could be readily destroyed by photodissociation

$$He_2^+ + h\nu \rightarrow He + He^+ \quad (22)$$

and by dissociative recombination

$$He_2^+ + e \rightarrow He + He \quad (23)$$

It is important to add at this point that the estimated abundance of He_2^+ is 20 orders of magnitude less than that of HeH^+ for $z < 1000$.[12]

He_2^+ could combine with H to give He_2H^+ and in turn to yield HeH^+:

$$He_2^+ + H \rightarrow [He_2H^+] \rightarrow He + HeH^+ \quad (24)$$

The spectral characteristics of He_2H^+ are discussed later in this article.

7 LiH^+ in early universe chemistry

Lithium was the first metallic atom/nucleus to be formed in the early Universe, and it was 10 orders of magnitude less in abundance than hydrogen. The protonated diatomic species LiH^+ was thought that could be formed through radiative association

$$Li^+ + H \rightarrow LiH^+ + h\nu \quad (25)$$

and with a minor contribution through

$$Li + H^+ \rightarrow LiH^+ + h\nu \quad (26)$$

while it could also be destroyed by dissociative recombination

$$LiH^+ + e \rightarrow Li + H \quad (27)$$

and by

$$LiH^+ + H \rightarrow Li^+ + H_2 \quad (28)$$

and

$$LiH^+ + H \rightarrow Li + H_2^+ \quad (29)$$

The proton transfer, eqn (29), is less likely to occur as it is highly endothermic. Lepp *et al.*[15] concluded that LiH^+ was more abundant than LiH for smaller redshifts ($z < 30$).

Lithium hydride and its ionic counterpart, LiH^+, have attracted for many years the interest of theorists and experimentalists. Below 3000 K the collisional excitation of rotational levels of the most abundant species, the hydrogen molecule, is negligible and therefore lithium hydride partners with their low-excitation temperatures and fast radiative decay become the most likely ones to be able to accomplish the role of coolants. Furthermore, these species have usually been taken to live longer than H_2. The possible presence of LiH^+ was first postulated by Dalgarno and Lepp[63] who suggested it to be formed by efficient ion-atom radiative association, eqn (26).

However, it was further noted that the abundance of LiH^+ could also be effectively reduced by an important destruction mechanism,

$$LiH^+ + H \rightarrow Li^+ + H_2 \quad (30)$$

a barrierless, exothermic gas-phase reaction, already indicated in eqn (28)[64,65] that forms hydrogen molecules from the abundant atomic H known to be present in that environment. Another important destruction mechanism was also suggested by Stancil *et al.*[66] and includes the charge-exchange depletion reaction,

$$LiH^+ + H \rightarrow Li + H_2^+ \quad (31)$$

and the charge-transfer reaction that contributes to the abundance of the neutral molecule

$$LiH^+ + H \rightarrow LiH + H^+ \quad (32)$$

However, these two reactions are unlikely to occur as they are both endoergic by 5.7 and 5.8 eV, respectively. The fully dissociative channel, *i.e.*, the three-body (3B) break-up process induced by collision (collision-induced dissociation (CID)), as suggested in our earlier work[64] would also be probable at low energies although it would not be important from the point of view of altering the LiH^+ abundances.

A careful analysis of various primordial molecules which are expected to be present in the early universe has led to the identification of LiH and LiH^+ as the best candidates that could have left their imprints on the Cosmic Background Radiation (CBR) *via* Doppler shift.[67,68] Primary and secondary anisotropies, in fact, could be produced from these molecules, *e.g.* see: ref. 69, 70. However, such findings strongly depend on their assumed abundances relative to the primary abundance of H. In the work published by some of us (FAG) in 2009 with Bovino *et al.*,[71] the authors were able to show from quantum calculations that LiH abundance (as suggested by Stancil *et al.*[66]) is strongly reduced by a destruction mechanism that should then lead to no erasing of primordial CBR anisotropies and no production of secondary anisotropies in the recombination era. When one now turns to the ionic LiH^+, however, besides its being important in the formation of the LiH molecules through the exchange reaction (LiH^+, H), it was found that it is

Open Access Article. Published on 17 August 2023. Downloaded on 09.08.2025 04:28:18.
This article is licensed under a Creative Commons Attribution-NonCommercial 3.0 Unported Licence.

a molecule which could have survived at low redshifts and could have left its imprint on the CBR, thanks to its large permanent dipole moment (as suggested by Dubrovich[67]).

Therefore, quantum reactive scattering calculations for the exothermic reaction of the LiH^+ molecular cation with hydrogen atom at the temperatures corresponding to the redshift values deemed to be important for the lithium chemistry in the early universe environment ($z < 400$) have been trying to establish from first principles the possible efficiency of the chemical routes to the depletion rates. The calculations described in ref. 71 found that the survival process for LiH^+ to be the most likely process at low-T, indicating that, because of specific features of their reactive PES[71] the two partners undergo essentially repulsive interaction at short range in the product region due to the marked increase of the products relative kinetic energy, while the more stable bound complex (LiH_2^+) is formed within a range of distances that correspond to the reactants region of interaction.

Furthermore, the depletion reaction mentioned before remains, however, an important reactive process that leads to the disappearance of LiH^+ cations initially formed during the recombination era. In other words, it was found from the quantum calculations of ref. 65 that the exothermic process is indeed the dominant reactive process that leads to density reduction for the cationic hydride. The LiH^+ partner is therefore expected, from the balancing role of the above two pathways, to remain present in the low-z period, thereby becoming able to contribute to molecular cooling processes during the post-recombination era. As the temperature increases, the 3B break-up process has been shown to become more important, as surmised by the calculations of ref. 72 thereby leading to the disappearance of the LiH^+ that survived the exothermic depletion reaction discussed before, hence leading to a reduction of its role as a coolant.

8 $LiHe^+$ formation in the ISM

Because of its large dipole moment and its low ionization potential, LiH has been considered for a long time a potential candidate for inducing spatial and/or spectral distortions of the Cosmic Background Radiation, as originally suggested a while ago by Dubrovich[67] and observationally tested by Maoli *et al.*[69] It is, in fact, its possible role as a molecular coolant of the primordial gas, because of its efficient radiative decay down its manifold of rotovibrational levels, that made its likely presence a very important issue in several earlier studies.[73] By the same token, other molecular species formed as cations after atomic ionization during gravitational collapse, *e.g.* LiH^+, HeH^+, HD^+ and $LiHe^+$, could also play a similar role as additional molecular coolants and their non-equilibrium level populations may also have left a possible signature in protogalactic clouds, imprinting spatial or spectral distortions in the CBR spectrum.[74]

A few years back some of us, *e.g.* see ref. 75, had carried out an extensive analysis *via* a series of quantum calculations to determine the relative role of several pathways to its formation and destruction within the chemical network acting at low redshift. As a matter of fact, in previous papers by Bovino *et al.*,[76,77] the photonic paths to the formation and destruction of $LiHe^+$ were examined in some detail, while in ref. 75 that work was further extended by adding the chemical paths presiding over its evolution, *i.e.*, the chemical reaction with hydrogen,

$$LiHe^+ + H \rightarrow LiH^+ + He \quad (33)$$

leading to its destruction, and the formation reaction from the lithium hydride cation:

$$LiH^+ + He \rightarrow LiHe^+ + H \quad (34)$$

The physical characteristics of the above reaction were discussed extensively in ref. 78. An additional path that was also considered in the above study is that driven by the presence of a residual electron fraction in the early universe (Stancil *et al.*[66]), *i.e.*, the fragmentation of the polar cation by the dissociative recombination process:

$$LiHe^+ + e^- \rightarrow LiHe^* \rightarrow Li + He + h\nu \quad (35)$$

a reaction that, from those extensive calculations, also turned out to be fairly efficient.

In the work reported in ref. 75 the authors analyzed in greater detail the variety of molecular processes, partly summarized above, which involve a usually poorly studied molecular cation, $LiHe^+$ ($^1\Sigma^+$), and which deal with its possible formation and destruction in the pregalactic gas through an extensive network of photon-induced and chemically driven processes. In the range of redshifts of interest, they carried out quantum calculations of chemical formation/destruction reactions which have never been considered before from realistic computational models and which have been reported above in eqn (33), (34) and (35).

The results of that study clearly showed the existence of the close competition between production and destruction pathways which however also turned out to have very similar efficiencies. Hence, the estimated abundances for $LiHe^+$, within z values from about 30 and 10, do not increase as highly as those found in the same study for LiH^+ and for HeH^+. Such findings therefore indicated from accurate calculations that the expected abundances, and hence the chemical role, of the above cation would not be as significant as that involving other, albeit just as simple, molecular cations.

9 The role of H_3^+ in Interstellar chemistry

Detected first in 1911 by J. J. Thompson,[79] H_3^+ was also detected along with HeH^+ and HeH_2^+ in a mass spectrograph by Hogness and Lunn[17] in 1925. It is the simplest two-electron-three-nuclei system one could think of and is a prototype for a 3-centre two-electron bond. Since it has an equilateral triangular geometry in its ground electronic state, it does not have a

 This journal is © the Owner Societies 2023

Open Access Article. Published on 17 August 2023. Downloaded on 09.08.2025 04:28:18.
This article is licensed under a Creative Commons Attribution-NonCommercial 3.0 Unported Licence.

permanent dipole moment and its rotational spectrum is not active in infrared or microwave. However, its bending motion is infrared active. This was predicted by *ab initio* calculations by Carney and Porter[80] in 1976 and verified in the laboratory by Oka[81] in 1980. That formed the basis for the detection of the species in ISM conditions in 1996.[7] Subsequent astronomical observations have shown that it is perhaps the most abundant molecular ionic species in dense molecular clouds (responsible for star formation) as well as in diffuse clouds.[82]

While an electron impact causes ionization of H_2 in a mass spectrometer, cosmic radiation is believed to be responsible for the ionization in molecular clouds.[9] H_2^+ reacts readily with the abundant H_2 and forms H_3^+ as mentioned earlier.

In the early universe, the H_3^+ formation was perhaps through the reaction of HeH^+ with H_2. It is considered the major coolant for the gravitationally condensing gas. Zicler *et al.*[83] estimated the k_{RA} for

$$HeH^+ + H_2 \rightarrow HeH_3^+ + h\nu, \quad \Delta E = -2.68 \text{ eV} \qquad (36)$$

to rise from 3.1×10^{-19} cm^3 molecule^{-1} s^{-1} at 10 K to 2.01×10^{-18} cm^3 molecule^{-1} s^{-1} at 100 K and to decline to 7.1×10^{-19} cm^3 molecule^{-1} s^{-1} at 500 K.

Once formed, H_3^+ facilitates proton transfer to atoms like He, C, N and O and molecules like CO, CN and N_2:

$$H_3^+ + He \rightarrow HeH^+ + H_2 \qquad (37)$$

$$H_3^+ + C \rightarrow CH^+ + H_2 \qquad (38)$$

$$H_3^+ + N \rightarrow NH^+ + H_2 \qquad (39)$$

$$H_3^+ + O \rightarrow OH^+ + H_2 \qquad (40)$$

$$H_3^+ + CO \rightarrow HCO^+ + H_2 \qquad (41)$$

$$H_3^+ + CN \rightarrow HCN^+ + H_2 \qquad (42)$$

$$H_3^+ + N_2 \rightarrow N_2H^+ + H_2 \qquad (43)$$

in dense molecular clouds.

H_3^+ seems to be quenched by the electrons arising from the photoionization of C in diffuse clouds:

$$H_3^+ + e \rightarrow H_2 + H \qquad (44)$$

The interconnection between He, H, H_2 and related ionic species is depicted in Fig. 2.

We must also point out here that the singly deuterated H_3^+, *i.e.* H_2D^+ has the virtue, akin to that of HD^+, that H_2D^+ is now provided by a permanent dipole moment. As a consequence of this structural change it can participate much more effectively as a molecular coolant than H_3^+, but its occurrence would be several orders of magnitude lower than that of H_3^+. Furthermore, one needs to distinguish between *o*- and *p*-H_2D^+ as well, thereby unduly complicating the establishment of realistic percentage densities involved in the chemical kinetics models of linked reaction processes.

10 The $HeHHe^+$ cation: a possible ionic entry in ISM networks

From the chemical viewpoint it is reasonable to assume that HeH^+ cation was the very first diatomic molecule formed in the early universe.[84] Larger helium containing cationic species (HHe_n^+ with n = 2–6) have been predicted, although not observed. Among them, the first term, $HeHHe^+$, has been discussed as a possible efficient emitter for observations at high-z[85] because of it large dipole transition moment under vibrational excitations, as we shall further discuss below.

This symmetric linear molecule has been studied both theoretically[36,86–88] and experimentally.[89] Using the CCSD(T)-F12/aug-cc-pVTZ level of theory, Fortenberry and Wiesenfeld[85] have investigated the possibility of $HeHHe^+$ formation through the insertion mechanism:

$$He_2^+ + H \rightarrow HeHHe^+(\text{singlet/triplet}) \qquad (45)$$

In addition to the formation of a symmetric linear $[HeHHe]^+$ in its ground electronic singlet state, there could be the formation of the first excited triplet state with a well defined isosceles triangular geometry and a dipole moment of 0.83 D. While the antisymmetric stretch and bending modes of the singlet $[HeHHe]^+$ would be infrared active, the rotational motion of the triplet state could be microwave active. There could be another route to the formation of $[HeHHe]^+$:

$$He_2^+ + H_2 \rightarrow HeHHe^+(\text{singlet}) + H \qquad (46)$$

Recent quantum inelastic scattering studies[90,91] of this molecule with He atoms show fairly large rate coefficients, compared to HeH^+ colliding with He and H,[37,92] under similar conditions, suggesting a possible energy dissipation process after the recombination era. With these results, modeling of the kinetic evolution of the early universe should realistically include $HeHHe^+$.[93]

11 Small C-bearing cations

The number of few-carbon atoms-containing cations which have come under observation in the interstellar environments, and which have been finally detected with an acceptable level of reliability, has certainly increased in the last few years. It is therefore useful for the present perspective article to report a few cases which have been spotted and analysed under different points of view to elucidate both their occurrence and their possible roles within the chemical networks which are being modelled within circunstellar envelopes (CSE) environments.

11.1 The CH^+: the smallest C-bearing cation

Due to their low dissociation energies, the molecules CN, CH^+ and CH are most frequently found in molecular clouds where dust provides shielding from the ambient radiation field. The current data are generally towards low-reddening objects, in contrast to many previous studies, which until recently had the aim of determining the conditions within normal

Open Access Article. Published on 17 August 2023. Downloaded on 09.08.2025 04:28:18.
This article is licensed under a Creative Commons Attribution-NonCommercial 3.0 Unported Licence.

and high-latitude molecular clouds or star-forming regions. The methylidyne ion CH^+ was among the first molecules detected in the interstellar medium (ISM).[94] For decades, CH^+ remained accessible only in absorption at 423.2 nm, restricting its investigation to the lines-of-sight (LOS) toward bright nearby stars. The CH^+ abundances observed in the local diffuse ISM are several orders of magnitude above the predictions of UV-driven steady-state models (see references in ref. 95), raising one of the most intractable puzzles in our understanding of the ISM. Unfortunately, the detection of the CH^+ ground-state rotational transitions has been prevented for a long time since CH^+ is a light molecule; its lowest rotational transition lies in the submillimetre range. Additionally, its high reactivity makes it difficult to isolate in laboratory experiments.[96] Only recently did successful experiments provide accurate frequency determinations.[97] Moreover, ground-based astronomical detection of $^{12}CH^+$ (1-0 emission) is prevented by its proximity to a strong atmospheric line of water vapor. The first detection of the CH^+ rotational lines (above j = 2-1) was achieved by ISO-LWS in the planetary nebula NGC7027 as in ref. 98. The CH^+ (1-0) line has been detected in emission and absorption with the Herschel/HIFI instrument in DR21 (see ref. 99) and, as spectrally unresolved lines with the Herschel/SPIRE FTS (see ref. 100), in emission in the Orion Bar and in absorption in two SFRs (see ref. 101). The ground-state transition of the isotopologue $^{13}CH^+$, at a frequency lower by $\sim$5 GHz, can be observed under exceptional atmospheric conditions and was detected in absorption toward SgrB2(M) and several massive SFRs of the inner Galaxy with the Atacama Pathfinder EXperiment (APEX) telescope and the Caltech Submillimeter Observatory (CSO) telescope (see ref. 102). The large observed abundances of CH^+ have always been a major puzzle of the diffuse interstellar chemistry, since the only reaction efficient enough to form this molecular ion would be:

$$C^+ + H_2 \rightarrow [CH^+] + H \quad (47)$$

turns out to be highly endothermic (E/k = 4640 K). This suggests that large amounts of suprathermal energy need to be deposited in the cold neutral medium. In the past, several scenarios have been investigated, including C-shocks (*e.g.* see ref. 103), turbulent interfaces between the warm and cold neutral medium[104] and regions of intermittent turbulent dissipation (TDR models, see ref. 95). While the reaction between C^+ and vibrationally excited H_2 could account for the large abundances of this cation in dense and highly illuminated photodissociation regions (PDR), this mechanism is found inefficient for the physical conditions of the diffuse ISM (Agundez *et al.*[105]). This riddle could be related to the observed excess of HCO^+ in the diffuse ISM (see references in ref. 106) because CH^+-rich environments with H_2 molecular fractions as low as 25% enhance the production of HCO^+ through the ion-neutral reaction chain

$$CH^+ + H_2 \rightarrow CH_2^+ + H \quad (48)$$

$$CH_2^+ + H_2 \rightarrow CH_3^+ + H \quad (49)$$

$$CH_3^+ + O \rightarrow HCO^+ + H_2 \quad (50)$$

The TDR code is a 1-dimensional model in which the chemical and thermal evolution of a turbulent dissipative burst – namely a magnetized vortex – is computed. The lifetime of the burst is controlled by the turbulent rate-of-strain a of the large scales. At any time, a large number of these tiny regions ($\sim$100 AU), altogether filling a small fraction of the entire LOS, are developing a transient warm chemistry triggered by both the viscous dissipation and the ion-neutral friction, where local CH^+ and HCO^+ abundances reach 10^{-6} and 3×10^{-7}, respectively.[95] A random LOS therefore samples three kinds of diffuse gas: (1) mainly the ambient medium in which the chemistry is driven by the UV radiation field, (2) the active vortices with a filling factor set by the energy transfer rate in the turbulent cascade and identified with a significant turbulent dissipation rate, and (3) the long-lasting relaxation stages where the gas previously heated cools down to its original state. Hence, the use of this model has suggested that the high abundances of CH^+ observed in various ISM environments could be explained within the framework of models where the chemistry chains include routes which are locally open to turbulent dissipation bursts (*i.e.* within TDR models as in ref. 106).

11.2 C_3H^+: a longer carbonaceous cation

Small hydrocarbon molecules play an important role in the astrochemistry of the interstellar and circumstellar medium since they are expected to be leading to the formation of large organic molecules and ultimately to polycyclic aromatic hydrocarbons (PAHs) and carbonaceous dust (*e.g.* see ref. 107 and 108). In UV-rich environments, like diffuse clouds and photodissociation regions (PDRs), they can also be considered as exceptional tracers of the interplay between PAH formation and their photo-destruction.[109] On the other hand, although small neutral hydrocarbons like C_3H_2 and C_2H are commonly used as probes for physical and chemical conditions in the interstellar medium (for references see ref. 110), observations of reactive carbocations, which are important intermediates in carbon astrochemistry (Wakelam *et al.* in ref. 111) have so far been limited to C^+ and CH^+ (*e.g.*: Nagy *et al.*[112]), mostly due to a lack of accurate laboratory spectroscopic work on the larger cationic species. More recent observational work[113] attributed a series of rotational emission lines observed at millimeter-wavelengths toward the Horsehead PDR to the carbocation C_3H^+. The identification was based on spectroscopic constants resulting from a fit of six (plus two tentatively) detected harmonically related rotational lines to a closed-shell linear-rotor Hamiltonian. The derived rotational constant B = 11.245 GHz agreed well with the value obtained from previous theoretical calculations of the closed-shell ($^1\Sigma^+$) isomeric ground state of the ion with this chemical composition. More recent laboratory experiments in a 4 K cryogenic ion trap (see ref. 114) were able to detect the line positions of four rotational transitions with a relative precision of 3×10^{-7}. These experimentally derived transition frequencies and related spectroscopic constants

Open Access Article. Published on 17 August 2023. Downloaded on 09.08.2025 04:28:18.
This article is licensed under a Creative Commons Attribution-NonCommercial 3.0 Unported Licence.

turned out to agree with those from the previous astronomical onservations, thereby unambiguously confirming the detection of this important carbonaceous cation and excluding its anionic variant suggested earlier on. More recent computational work has also been directed to the study of the interaction of this cation with He atoms (see ref. 115) whereby the corresponding collisional rate coefficients for its rotational transitions were reported for temperatures up to about 100 K. Not yet specific chemical routes have been discussed or verified to explain the formation of this cations, thus leaving fairly open the general suggestions on the preparation of more complex carbon-bearing positive ions in interstellar environments.

12 Cations with higher metallicity

While the elements formed in the early Universe were only He, H, D and Li, subsequent events in the evolution of the Universe led to the formation of stars and galaxies and in the process higher elements up to iron (atomic number = 26) in the periodic table.[116,117] Elements with atomic number >26 seem to have been formed only as a result of supernovae. Understandably all those elements could also form cations either by themselves or also when in associaton with other elements in the periodic table.

Without going into the details of stellar nucleosynthesis, it is important to point out that in general there seems to be enough C, N and O in the Sun, playing an important role in the helium formation as the hydrogen ''burns''. Atoms/ions of many other elements are spewed out from a variety of stars during their stellar dynamics and the ISM appears to contain several cations, anions and neutral molecular species. For a recent review on the subject, the reader is referred to ref. 10.

We mention here the discovery of NO^+ through its j = 2-1 line[118] and $HCNH^+$ through its j = 3-2 line.[119] The former is special in that it contains N as well as O. The latter is special because it is the protonated form of HCN (vital for the formation of life giving molecules) and could be formed through

$$HCN + HCO^+ \rightarrow HCNH^+ + CO \quad (51)$$

under ''warm'' (T = 27 K) conditions. The characteristics and the significance of HCO^+ are discussed further below. Under cold (T = 10 K) conditions, it appears that $HCNH^+$ is formed through the pathway

$$HCN^+(HNC^+) + H_2 \rightarrow HCNH^+ + H \quad (52)$$

and destroyed by the dissociative recombination:

$$HCNH^+ + e \rightarrow HCN + H;HNC + H \quad (53)$$

$$HCNH^+ + e \rightarrow CN + H + H \quad (54)$$

HCN^+ (HNC^+) itself is formed presumably from the reaction

$$CN + H_3^+ \rightarrow HCN^+(HNC^+) + H_2 \quad (55)$$

12.1 A small polyatomic partner: H_3O^+

Predicted to be present in dense molecular clouds by Herbst and Klemperer[6] in 1973, H_3O^+ was first observed astronomically in 1986 by Wootten *et al.*[120] and Hollis *et al.*[121] A review of subsequent observations and the characteristics of the species is given in the work of Demes *et al.*[122] It is believed that the observation of H_3O^+ in ISM is adequate proof for the existence of H_2O in the same environment. Dissociative recombination of the former leads to the latter:

$$H_3O^+ + e \rightarrow H_2O + H \quad (56)$$

The mechanism of formation of H_3O^+ in molecular clouds was discussed by Demes *et al.*[123] The understanding is that in diffuse clouds, H_3O^+ is formed through the route,

$$OH^+ + H_2 \rightarrow H_2O^+ + H \quad (57)$$

$$H_2O^+ + H_2 \rightarrow H_3O^+ + H \quad (58)$$

The OH^+ itself could be formed through the reaction[124]

$$O^+ + H_2 \rightarrow OH^+ + H \quad (59)$$

Deep within dense molecular clouds, H_3O^+ plays a central role in producing OH^+ through the reaction

$$H_3O^+ + O \rightarrow H_2 + OH^+ \quad (60)$$

Demes *et al.*[122,123] reported the results of quantum mechanical close coupling calculations using a 5D *ab initio* PES[125] in the form of rotational de-excitation cross sections for *o*-/*p*-H_3O^+ in collision with *o*-/*p*-H_2

$$H_3O^+(j_1) + H_2(j_2) \rightarrow H_3O^+(j_1') + H_2(j_2') \quad (61)$$

for a range of E_{trans}. They reported many Feshbach and shape resonances, particularly at lower energies. Interestingly, the reported rate coefficients were comparable in magnitude for *o*-H_3O^+ and *p*-H_3O^+ for T in the range 10–300 K. They were slightly less than 10^{-9} cm^3 molecule^{-1} s^{-1} for $\Delta j_1 = -1$ transitions and decreased to 10^{-10} cm^3 molecule^{-1} s^{-1} for larger Δj_1 transitions and changed very little in going from *p*-H_2 to *o*-H_2 as the collision partner. The k values decreased slightly (in the logarithmic scale) in going from T = 10 to 100 K and remained nearly flat for higher T.

12.2 The HCO^+ cation

One of the fundamental questions concerning the chemistry in circumstellar envelopes of evolved stars is the role of ion–molecule reactions. Such reactions are thought to be significant contributors to molecule formation in the outer part of the envelope, where they are initiated by either cosmic rays or UV photoionization.

One molecular ion that has been searched for decades in circumstellar material has been HCO^+. This species is thought to be critical in the ion–molecule schemes because it is expected to be formed directly from H_3^+ and CO:

$$H_3^+ + CO \rightarrow HCO^+ + H_2 \quad (62)$$

Open Access Article. Published on 17 August 2023. Downloaded on 09.08.2025 04:28:18.
This article is licensed under a Creative Commons Attribution-NonCommercial 3.0 Unported Licence.

HCO^+ in fact is observed in virtually all phases of the dense interstellar medium, including molecular clouds, planetary nebulae, and diffuse clouds, as well as in comets.[126] However, the presence of HCO^+ in IRC + 10216, the best-studied circumstellar shell, has been debated for years. More recently, Millimeter-wave observations of HCO^+ have been conducted toward oxygen-rich circumstellar envelopes, as well as IRC + 10216, using the facilities of the Arizona Radio Observatory (ARO).[127] Hence, the $j = 1 \rightarrow 0$ and the $2 \rightarrow 1$ transitions of this cation were measured with the ARO 12m. antenna, while the $j = 3 \rightarrow 2$ and $4 \rightarrow 3$ lines were observed using the ARO Sub-Millimeter Telescope.[127] Additionally, the HCO^+ cation was detected toward the supergiant NML Cyg and the asymptotic giant branch (AGB) stars IK Tau, TX Cam, and W Hya in at least two transitions. The $j = 2 \rightarrow 1$ and $3 \rightarrow 2$ lines of this ion were also detected toward IRC + 10216, confirming the identification of HCO^+ in this object.[127]

Chemical models suggest that HCO^+ is formed in the outer envelopes of stars *via* two primary synthetic routes.[128] One pathway is from the simple protonation reaction of CO, as is thought to occur in molecular clouds; and we mentioned earlier in this Subsection. Another pathway is *via* H_2O:

$$C^+ + H_2O \rightarrow HCO^+ + H \quad (63)$$

The destruction of HCO^+ is thought to occur *via* electron dissociative recombination, or proton transfer to water to create H_3O^+.[128] Based on these pathways, fractional abundances for HCO^+ have been computed by several models as extensively discussed in ref. 127, where it was concluded that HCO^+ appears to be a common species in oxygen-rich circumstellar shells, both of supergiants and AGB stars. It is also present in the carbon-rich envelope of IRC + 10216, but in much lower concentration. The abundance of HCO^+ appears to be best correlated with that of water in stellar envelopes; however, its production from CO must also play a significant role. The abundance of HCO^+ also appears from that study to be inversely proportional to the mass-loss rate, although they concluded that additional sources warrant investigation to further examine such trends. These observations also suggest that ion–molecule reactions must be occurring in circumstellar gas at some level. It follows, in fact, that other ions such as H_3O^+ may be detectable in O-rich shells.

It is also interesting to note at this point that a recent computational study[129] has investigated the possibility that, in cold galactic molecular clouds, dust grains coated by icy mantles are prevalently charged negatively because of the capture of the electrons in the gas. It would therefore follow that the interaction of the charged grains with gaseous cations could efficiently neutralize them thereby taking them off the chemical chain of likely reactions.[129] More specifically, by means of electronic structure calculations, the energy and the structure of all possible product species once the HCO^+ ion adsorbs on water clusters holding an extra electron were searched and characterized. Among the possible situations considered, those results indicated that spontaneous formation of the HCO radical by electron transfer is energetically the most favorable path, although no actual rates were obtained. Accordingly, they suggested that interstellar grain particles could act as a reservoir of electrons, triggering electron transfer processes with the molecular cations, like HCO^+, adsorbed on such grain particles, thereby modifying the overall abundance of this specific molecular ion in molecule-rich Circumstellar Envelopes.

12.3 Mg-Bearing cations

Radiative association seems to play an important role in bringing cations together with neutrals with the rates governed by Langevin capture. See for example, the recent report of Cernicharo *et al.*[130] on the discovery of MgC_4H^+, MgC_3N^+, MgC_6H^+ and MgC_5N^+. These findings are particularly relevant since polytomic, metal-containig molecules have been detected only toward the Circumstellar Envelopes (CSEs) of fully evolved stars, while simpler diatomic species containing Al, Na or K attached to a halogen atom have been detected in the earlier Carbon star envelope IRC + 10216[131] where these species are formed in the hot inner parts of the envelope, closer to the stellar core. More recently, the only metal that was found to lead to molecular formations with more than three atoms in the IRC + 10216 has been magnesium (see ref. 132–134). It is only in very recent publications, like ref. 130, that the presence of Mg-containing cations has been put forward and its formation routes explored with quantum calculations. In particular, the various cations listed above have been suggested to be formed by radiative association between Mg^+ and the corresponding neutral radicals like C_4H, C_3N, C_6H and C_5N, while also being destroyed *via* dissociative recombination with electrons and by reaction with atomic hydrogen.

Comparison of the corresponding association rate coefficients within a larger chemical model for the formation of the initial radical species and the Mg cation indeed suggested that the radiative asociation paths involving the atomic cation of the metal species with the molecular radicals is a realistic process for explaining the appearance of molecular cations with heavier metal atoms. Such findings therefore constitute a very recent confirmation that molecular cations in different ISM environments can indeed be formed with heavier atoms than previously expected.[130]

13 Conclusions

In the present perspective article, we have focussed on a specific subset of a variety of molecular cations, involving combinations of the most abundant light atoms present in ISM environments, *i.e.* H and He. Because of the all-present effects from starlight, it turns out that these small cations can be efficiently formed but also easily destroyed by recombination processes involving the free electrons in that same environments or in other regions of the Dark and of the Diffuse Molecular Clouds. Besides cations involving H and He, we have also looked at the formation of cations involving lithium partners, one of the important atomic species which is

 This journal is © the Owner Societies 2023

Open Access Article. Published on 17 August 2023. Downloaded on 09.08.2025 04:28:18.
This article is licensed under a Creative Commons Attribution-NonCommercial 3.0 Unported Licence.

considered to be relevant in the high-z regions of the early universe conditions. Additionally, we discuss very recently detected Mg-bearing molecular cations which constitute current examples of molecular ions that involve heavier metal species.

The examples in this work clearly point at a surprisingly varied presence of molecular cations in the same interstellar environments where also neutral molecules and molecular anions are detected, thus suggesting that chemical routes involving positive ions as possible partners, are indeed a significant aspect of the ISM chemistry.

Before closing, we would like to re-iterate that many of the ion–molecule reactions mentioned in this perspective article are exothermic and face no potential energy barrier. In addition, there is a long-range attraction that goes as R^{-4} that is particularly important at low temperatures. Langevin cross sections lead to rate coefficients of the order of 10^{-9} cm^3 molecule^{-1} s^{-1}. In comparison, dissociative (electron) recombination has k values of the order of 10^{-7} cm^3 molecule^{-1} s^{-1}.

In spite of the fact that k values which deal with several exothermic reactions are only weakly T-dependent, Herbst[135] has pointed out that they can have a U-shaped T-dependence at very low temperatures. Rotationally inelastic rate coefficients for $\Delta j = \pm 1, \pm 2$ (depending upon the molecule being heteronuclear or homonuclear) transitions are also of the order of 10^{-9} cm^3 molecule^{-1} s^{-1}. For larger Δj transitions, the k values decrease exponentially with an increase in the energy gap between the initial and the final rotational states. The k values for the vibrationally inelastic transitions ($\Delta v = \pm 1$) are at least an order of magnitude lower than those for the rotationally inelastic ($\Delta j = \pm 1, \pm 2$) transitions for a given molecular (ionic) species.

Although the k values for the formation of di-/tri-/polyatomic molecular cations by radiative association are often estimated to be $\leq 10^{-15}$ cm^3 molecule^{-1} s^{-1}, way below the k-values mentioned above, they are still expected to play a significant role at extremely low densities (in the absence of any third body), as it is the case in the early universe conditions.

In conclusion, the small cations examined in this perspective indicate that their formation in the ISM conditions are linked to a broad range of kinetic mechanisms that take advantage of the presence of efficient long-range interaction forces and of the efficient coupling which they generate for both reactive and state-changing processes.

Conflicts of interest

There are no conflicts to declare.

Acknowledgements

F. A. G. acknowledge the support from the Computer Center of the University of Innsbruck. L. G.-S. further acknowledges the financial support by Ministerio de Ciencia e Innovación (Spain) MCIN/AEI/10.13039/501100011033 (Refs. PID2020-113147GA-I00 and PID2021-122839NB-I00).

References

1 F. Le Petit, E. Roueff and E. Herbst, *Astron. Astrophys.*, 2004, **417**, 993.
2 T. P. Snow and A. N. Witt, *Astrophys. J.*, 1996, **468**, L65.
3 D. A. Williams and E. Herbst, *Surf. Sci.*, 2002, **500**, 823.
4 A. Li and B. T. Draine, *Astrophys. J.*, 2001, **554**, 778.
5 E. Herbst, *J. Phys.: Conf. Ser.*, 2005, **4**, 17–25.
6 E. Herbst and W. Klemperer, *Astrophys. J.*, 1973, **185**, 505.
7 T. R. Geballe and T. Oka, *Nature*, 1996, **384**, 334.
8 S. Petrie and D. K. Bohme, *Mass Spectrom. Rev.*, 2007, **26**, 258–280.
9 M. Larsson, W. D. Geppert and G. Nyman, *Rep. Prog. Phys.*, 2012, **75**, 066901.
10 A. G. G. M. Tielens, *Rev. Mod. Phys.*, 2013, **85**, 1021–1081.
11 D. Galli and F. Palla, *Astron. Astrophys.*, 1998, **335**, 403–420.
12 D. Galli and F. Palla, *Annu. Rev. Astron. Astrophys.*, 2013, **51**, 163–206.
13 C. E. Moore, *Natl. Bur. Stand.*, 1970, 34.
14 T. Hartquist and D. Williams, *The Molecular Astrophysics of Stars and Galaxies*, Clarendon Press, 1998.
15 S. Lepp, P. C. Stancil and A. Dalgarno, *J. Phys. B: At., Mol. Opt. Phys.*, 2002, **35**, R57–R80.
16 M. Jurek, V. Špirko and W. Kraemer, *Chem. Phys.*, 1995, **193**, 287–296.
17 T. R. Hogness and E. G. Lunn, *Phys. Rev.*, 1925, **26**, 44.
18 R. Güsten, H. Wiesemeyer, D. Neufeld, K. M. Menten, U. U. Graf, K. Jacobs, B. Klein, O. Ricken, C. Risacher, J. Stutzki and S. Arnouts, *Nature*, 2019, **568**, 357–359.
19 D. A. Neufeld, M. Goto, T. R. Geballe, R. Güsten, K. M. Menten and H. Wiesemeyer, *Astrophys. J.*, 2020, **894**, 37.
20 B. Zygelman and A. Dalgarno, *Astrophys. J.*, 1990, **365**, 239.
21 W. Kraemer, V. Špirko and M. Jurek, *Chem. Phys. Lett.*, 1995, **236**, 177–183.
22 S. Adhikari, M. Baer and N. Sathyamurthy, *Int. Rev. Phys. Chem.*, 2022, **41**, 49–93.
23 D. De Fazio, *Phys. Chem. Chem. Phys.*, 2014, **16**, 11662.
24 M. M. Schauer, S. R. Jefferts, S. E. Barlow and G. H. Dunn, *J. Chem. Phys.*, 1989, **91**, 4593.
25 O. Novotný, P. Wilhelm, D. Paul, Á. Kálosi, S. Saurabh, A. Becker, K. Blaum, S. George and J. Göck, *et al.*, *Science*, 2019, **365**, 676–679.
26 R. C. Forrey, J. F. Babb, E. D. S. Courtney, R. McArdle and P. C. Stancil, *Astrophys. J.*, 2020, **898**, 86.
27 E. D. S. Courtney, R. C. Forrey, R. T. McArdle, P. C. Stancil and J. F. Babb, *Astrophys. J.*, 2021, **919**, 70.
28 Z. Karpas, V. Anicich and W. T. Huntress, *J. Chem. Phys.*, 1979, **70**, 2877.
29 N. G. Adams, D. K. Bohme and E. E. Ferguson, *J. Chem. Phys.*, 1970, **52**, 5101–5105.
30 K. R. Ryan and I. G. Graham, *J. Chem. Phys.*, 1973, **59**, 4260–4271.
31 J. A. Rutherford and D. A. Vroom, *J. Chem. Phys.*, 1973, **59**, 4561–4562.
32 G. Gioumousis and D. P. Stevenson, *J. Chem. Phys.*, 1958, **29**, 294–299.

Open Access Article. Published on 17 August 2023. Downloaded on 09.08.2025 04:28:18.
This article is licensed under a Creative Commons Attribution-NonCommercial 3.0 Unported Licence.

33 R. Johnsen and M. A. Biondi, *J. Chem. Phys.*, 1974, **61**, 2112–2115.
34 O. Orient, *Chem. Phys. Lett.*, 1977, **52**, 264–269.
35 L. P. Theard and W. T. Huntress, *J. Chem. Phys.*, 1974, **60**, 2840.
36 A. N. Panda and N. Sathyamurthy, *J. Phys. Chem. A*, 2003, **107**, 7125.
37 B. Desrousseaux and F. Lique, *J. Chem. Phys.*, 2020, **152**, 74303.
38 F. A. Gianturco, K. Giri, L. González-Sánchez, E. Yurtsever, N. Sathyamurthy and R. Wester, *J. Chem. Phys.*, 2021, **154**, 054311.
39 K. Giri, L. González-Sánchez, R. Biswas, E. Yurtsever, F. A. Gianturco, N. Sathyamurthy, U. Lourderaj and R. Wester, *J. Phys. Chem. A*, 2022, **126**, 2244–2261.
40 F. A. Gianturco, K. Giri, L. González-Sánchez, E. Yurtsever, N. Sathyamurthy and R. Wester, *J. Chem. Phys.*, 2021, **155**, 154301.
41 J. R. Hamilton, A. Faure and J. Tennyson, *MNRAS*, 2016, **455**, 3281.
42 B. Balta, F. A. Gianturco and F. Paesani, *Chem. Phys.*, 2000, **254**, 215–229.
43 F. Mrugała and W. P. Kraemer, *J. Chem. Phys.*, 2005, **122**, 224321.
44 M. Hernández Vera, F. A. Gianturco, R. Wester, H. da Silva Jr., O. Dulieu and S. Schiller, *J. Chem. Phys.*, 2017, **146**, 124310.
45 W. A. Chupka and M. E. Russell, *J. Chem. Phys.*, 1968, **49**, 5426.
46 W. A. Chupka, J. Berkowitz and M. E. Russell, *6th Int. Conf. on the Physics of Electronic and Atomic Collisions*, 1969, **ICPEAC VI**, 71.
47 J. C. Polanyi, N. Sathyamurthy and J. L. Schreiber, *Chem. Phys.*, 1977, **24**, 105–110.
48 C. Gayatri and N. Sathyamurthy, *Chem. Phys.*, 1980, **48**, 227–235.
49 I. Iskandarov, F. A. Gianturco, M. Hernandez Vera, R. Wester, H. da Silva and O. Dulieu, *Eur. Phys. J. D*, 2017, **71**, 141.
50 C. N. Ramachandran, D. De Fazio, S. Cavalli, F. Tarantelli and V. Aquilanti, *Chem. Phys. Lett.*, 2009, **469**, 26.
51 S. Schiller, I. Kortunov, M. H. Vera, F. A. Gianturco and H. da Silva, *Phys. Rev. A*, 2017, **95**, 043411.
52 M. H. Vera, R. Wester and F. A. Gianturco, *J. Phys. B: At., Mol. Opt. Phys.*, 2018, **51**, 014004.
53 A. K. Tiwari, A. N. Panda and N. Sathyamurthy, *J. Phys. Chem. A*, 2006, **110**, 389–395.
54 F. Mrugała, V. Špirko and W. P. Kraemer, *J. Chem. Phys.*, 2003, **118**, 10547.
55 A. Carrington, *Science*, 1996, **274**, 1327–1331.
56 A. Carrington, D. I. Gammie, A. M. Shaw and S. M. Taylor, *Chem. Phys. Lett.*, 1996, **262**, 598–602.
57 M. Meuwly and J. M. Hutson, *MNRAS*, 1999, **302**, 790–792.
58 D. I. Gammie, J. C. Page and A. M. Shaw, *J. Chem. Phys.*, 2002, **116**, 6072–6078.
59 D. G. Hopper, *J. Chem. Phys.*, 1980, **73**, 3289–3293.
60 S. Ravi, S. Mukherjee, B. Mukherjee, S. Adhikari, N. Sathyamurthy and M. Baer, *Mol. Phys.*, 2021, **119**, e1811907.
61 O. Asvany, S. Schlemmer, A. van der Avoird, T. Szidarovszky and A. G. Császár, *J. Mol. Spect.*, 2021, **377**, 111423.
62 D. Koner, J. C. S. V. Veliz, A. V. D. Avoird and M. Meuwly, *Phys. Chem. Chem. Phys.*, 2019, **21**, 24976–24983.
63 A. Dalgarno and S. Lepp, in *Astrochemistry*, ed. M. S. Vardya and S. P. Tarafdar, D, 1987.
64 E. Bodo, F. A. Gianturco, R. Martinazzo and M. Raimondi, *J. Phys. Chem. A*, 2001, **105**, 10986.
65 S. Bovino, T. Stoecklin and F. A. Gianturco, *Astrophys. J.*, 2010, **708**, 1560.
66 P. C. Stancil, S. Lepp and A. Dalgarno, *Astrophys. J.*, 1996, **458**, 401.
67 V. K. Dubrovich, *J. Astron. Lett.*, 1993, **19**, 53.
68 P. de Bernardis, *Astron. Astrophys.*, 1993, **269**, 1.
69 R. Maioli, *Astrophys. J.*, 1996, **457**, 1.
70 M. Signore, *Asron. Lett. Commun.*, 1997, **35**, 349.
71 S. Bovino, M. Wernli and F. A. Gianturco, *Astrophys. J.*, 2009, **699**, 383.
72 I. Pino, R. Martinazzo and G. F. Tantardini, *Phys. Chem. Chem. Phys.*, 2008, **10**, 5545.
73 E. Bougleux and D. Galli, *MNRAS*, 1997, **288**, 638.
74 D. R. G. Schleicher, D. Galli, F. Palla, M. Camenzind, R. S. Klessen, M. Bartelmann and S. C. O. Glover, *Astron. Astrophys.*, 2008, **490**, 521.
75 S. Bovino, R. Curik, D. Galli, M. Tacconi and F. A. Gianturco, *Astrophys. J.*, 2012, **752**, 19.
76 S. Bovino, M. Tacconi and F. Gianturco, *Astrophys. J.*, 2011, **740**, 101.
77 S. Bovino, M. Tacconi and F. A. Gianturco, *Astrophys. J.*, 2012, **748**, 150.
78 M. Tacconi, S. Bovino and F. A. Gianturco, *Phys. Chem. Chem. Phys.*, 2012, **14**, 637.
79 J. J. Thomson, *London, Edinburgh Dublin Philos. Mag. J. Sci.*, 1911, **21**, 225–249.
80 G. Carney and R. Porter, *J. Chem. Phys.*, 1976, **65**, 3547–3565.
81 T. Oka, *Phys. Rev. Lett.*, 1980, **45**, 531–534.
82 T. Oka, *Proc. Natl. Acad. Sci. U. S. A.*, 2006, **103**, 12235–12242.
83 E. Zicler, O. Parisel, F. Pauzat, Y. Ellinger, M.-C. Bacchus-Montabonel and J.-P. Maillard, *Astron. Astrophys.*, 2017, **607**, A61.
84 R. C. Fortenberry, *Chem*, 2019, **5**, 1028–1030.
85 R. C. Fortenberry and L. Wiesenfeld, *Molecules*, 2020, **25**, 2183.
86 R. D. Poshusta, J. A. Haugen and D. F. Zetik, *J. Chem. Phys.*, 1969, **51**, 3343–3351.
87 I. Baccarelli, F. A. Gianturco and F. Schneider, *J. Phys. Chem. A*, 1997, **101**, 6054–6062.
88 S. T. Kim and J. S. Lee, *J. Chem. Phys.*, 1999, **110**, 4413–4418.
89 M. Töpfer, A. Jensen, K. Nagamori, H. Kohguchi, T. Szidarovszky, A. G. Császár, S. Schlemmer and O. Asvany, *Phys. Chem. Chem. Phys.*, 2020, **22**, 22885–22888.

Open Access Article. Published on 17 August 2023. Downloaded on 09.08.2025 04:28:18.
This article is licensed under a Creative Commons Attribution-NonCommercial 3.0 Unported Licence.

90 L. González-Sánchez, E. Yurtsever, R. Wester and F. A. Gianturco, *J. Phys. Chem. A*, 2021, **125**, 3748–3759.
91 O. Denis-Alpizar, L. D. Cabrera-González, D. Páez-Hernández and R. Pino-Rios, *ACS Earth Space Chem.*, 2022, **6**, 1924–1929.
92 F. A. Gianturco, K. Giri, L. González-Sánchez, E. Yurtsever, N. Sathyamurthy and R. Wester, *J. Chem. Phys.*, 2021, **154**, 54311.
93 S. Bovino and D. Galli, *Science*, 2019, **365**, 639.
94 A. Douglas and G. Herzberg, *Astrophys. J.*, 1941, **94**, 381.
95 B. Godard, E. Falgarone and G. Pineau des Forets, *Astron. Astrophys.*, 2009, **495**, 847.
96 J. Pearson and B. Drouin, *Astrophys. J.*, 2006, **647**, L83.
97 T. Amano, *Astrophys. J.*, 2010, **716**, L1.
98 J. Cernicharo, X.-W. Liu and E. Gonzalez-Alfonso, *et al.*, *Astrophys. J.*, 1997, **483**, L65.
99 E. Falgarone, V. Ossenkopf and M. Gerin, *et al.*, *Astron. Astrophys.*, 2010, **518**, L118.
100 M. Griffin, A. Abergel and A. Abreu, *et al.*, *Astron. Astrophys.*, 2010, **518**, L3.
101 D. Naylor, E. Dartois and E. Habart, *et al.*, *Astron. Astrophys.*, 2010, **518**, L117.
102 E. Falgarone, T. J. Phillips and J. C. Pearson, *Astrophys. J.*, 2005, **634**, L149.
103 D. Flower and G. Pineau des Forets, *MNRAS*, 1998, **297**, 1182.
104 P. Lesaffre, M. Gerin and P. Hennebelle, *Astron. Astrophys.*, 2007, **469**, 949.
105 M. Agundez, J. Goicoechea and J. Cernicharo, *et al.*, *Astrophys. J.*, 2010, **713**, 662.
106 B. Godard, E. Falgarone, M. Gerin, P. Hily-Blant and M. DeLuca, *Astron. Astrophys.*, 2010, **520**, A20.
107 R. Bettens and E. Herbst, *Astrophys. J.*, 1997, **478**, 585.
108 A. Tielens, *Annu. Rev. Astron. Astrophys.*, 2008, **46**, 289.
109 J. Pety, D. Teyssier and D. Fosse, *et al.*, *Astron. Astrophys.*, 2005, **435**, 885.
110 D. Teyssier, D. Fosse and M. Gerin, *et al.*, *Astron. Astrophys.*, 2004, **417**, 135.
111 V. Wakelam, I. Smith and E. Herbst, *et al.*, *SSRv*, 2010, **156**, 13.
112 Z. Nagy, F. Van der Tak and V. Ossenkopf, *et al.*, *Astron. Astrophys.*, 2013, **550**, A96.
113 J. Pety, P. Gratier and V. Guzman, *et al.*, *Astron. Astrophys.*, 2012, **548**, A68.
114 S. Brueken, L. Kluge, A. Stoffels, O. Asvany and S. Schlemmer, *ApJL*, 2014, **783**, L4.
115 S. Chhabra and D. Kumar, *MNRAS*, 2020, **494**, 5675–5681.
116 E. M. Burbidge, G. R. Burbidge, W. A. Fowler and F. Hoyle, *Rev. Mod. Phys.*, 1957, **29**, 547–650.
117 G. Wallerstein, I. Iben, P. Parker, A. M. Boesgaard, G. M. Hale, A. E. Champagne, C. A. Barnes, F. Käppeler, V. V. Smith, R. D. Hoffman, F. X. Timmes, C. Sneden, R. N. Boyd, B. S. Meyer and D. L. Lambert, *Rev. Mod. Phys.*, 1997, **69**, 995–1084.
118 J. Cernicharo, S. Bailleux, E. Alekseev, A. Fuente, E. Roueff, M. Gerin, B. Tercero, S. P. T. No Morales, N. Marcelino, R. Bachiller and B. Lefloch, *Astrophys. J.*, 2014, **795**, 40.
119 F. Fontani, L. Colzi, E. Redaelli, O. Sipilä and P. Caselli, *Astron. Astrophys.*, 2021, **653**, A45.
120 A. Wootten, F. Boulanger, M. Bogey, F. Combes, P. J. Encrenaz, M. Gerin and L. Ziurys, *Astron. Astrophys.*, 1986, **166**, L15.
121 J. M. Hollis, E. B. Churchwell, E. Herbst and F. C. D. Lucia, *Nature*, 1986, **322**, 524.
122 S. Demes, F. Lique, A. Faure and F. F. S. van der Tak, *MNRAS*, 2023, **518**, 3593.
123 S. Demes, F. Lique, A. Faure, F. F. S. van der Tak, C. Rist and P. Hily-Blant, *MNRAS*, 2022, **509**, 1252.
124 D. Hollenbach, M. J. Kaufman, D. Neufeld, M. Wolfire and J. R. Goicoechea, *Astrophys. J.*, 2012, **754**, 105.
125 S. Demes, F. Lique, A. Faure and C. Rist, *J. Chem. Phys.*, 2020, **153**, 094301.
126 S. N. Milam, C. Savage, L. Ziurys and S. Wyckroff, *Astrophys. J.*, 2004, **615**, 1054.
127 R. L. Pulliam, J. Edwards and L. Ziurys, *Astrophys. J.*, 2011, **743**, 36.
128 M. Agundez and J. Cernicharo, *Astrophys. J.*, 2006, **650**, 374.
129 A. Rimola, C. Ceccarelli, N. Balucani and P. Ugliengo, *Front. Astron. Space Sci.*, 2021, **8**, 1.
130 J. Cernicharo, C. Cabezas, J. R. Pardo, M. Agúndez, O. Roncero, B. Tercero, N. Marcelino, M. Guélin, Y. Endo and P. de Vicente, *Astron. Astrophys.*, 2023, **672**, L13.
131 J. Cernicharo and M. Guelin, *Astron. Astrophys.*, 1987, **183**, L10.
132 K. Kawaguchi, E. Kagi and T. Hirano, *Astrophys. J.*, 1993, **406**, L39.
133 P. B. Changala, H. Gupta and J. Cernicharo, *Astrophys. J.*, 2022, **940**, L42.
134 J. Cernicharo, C. Cabezas and J. Pardo, *Astron. Astrophys.*, 2019, **630**, L2.
135 E. Herbst, *Front. Astron. Space Sci.*, 2021, **8**, 776942.